archives
of thermodynamics
Vol. **44**(2023), No. 3, 119–141
DOI: 10.24425/ather.2023.147540

Investigation of thermal-flow characteristics of the minichannel heat exchanger of variable louvers height

ARTUR ROMANIAK*
MICHAŁ JAN KOWALCZYK
MARCIN ŁĘCKI
ARTUR GUTKOWSKI
GRZEGORZ GÓRECKI

Lodz University of Technology, Żeromskiego 116, 90-924 Łódź, Poland

Abstract The numerical simulation of the heat transfer in the flow channels of the minichannel heat exchanger was carried out. The applied model was validated on the experimental stand of an air heat pump. The influence of louver heights was investigated in the range from 0 mm (plain fin) to 7 mm (maximum height). The set of simulations was prepared in Ansys CFX. The research was carried out in a range of air inlet velocities from 1 to 5 m/s. The values of the Reynolds number achieved in the experimental tests ranged from 93 to 486. The dimensionless factors, the Colburn factor and friction factor, were calculated to evaluate heat transfer and pressure loss, respectively. The effectiveness of each louver height was evaluated using the parameter that relates to the heat transfer and the pressure drop in the airflow. The highest value of effectiveness (1.53) was achieved by the louver height of 7 mm for the Reynolds number of around 290.

Keywords: CFD; Heat transfer; Heat pump; Louvered fins; Minichannel heat exchanger

Nomenclature

A	–	airside area of the heat exchanger, m^2
A_c	–	minimum free flow area, m^2
c_p	–	air specific heat, J/(kg K)

*Corresponding Author. Email: artur.romaniak@dokt.p.lodz.pl

www.czasopisma.pan.pl PAN POLSKA AKADEMIA NAUK www.journals.pan.pl

F_d	–	flow depth, mm
F_p	–	fin pitch, mm
f	–	friction factor
H	–	fin height, mm
h	–	mean value of heat transfer coefficient, W/(m^{2}K)
JF	–	parameter related to heat transfer and pressure drop in airflow
j	–	Colburn factor
j_{ref}, f_{ref}	–	reference values of j and f factors (for $L_h = 0$ mm)
L_a	–	louver angle, $^\circ$
L_h	–	louver height, mm
L_l	–	louver length, mm
L_p	–	louver pitch, mm
Nu	–	Nusselt number
Pr	–	Prandtl number
p_{in}	–	air pressure at the inlet to the evaporator, Pa
p_{out}	–	air pressure at the outlet of the evaporator, Pa
Re	–	Reynolds number
T_{in}	–	mean value of air temperature at the inlet to the evaporator, K
T_{out}	–	mean value of air temperature at the evaporator outlet, K
v_{ave}	–	mean value of airstream velocity in the air MCHE channel, m/s
v_{fr}	–	mean value of the frontal velocity of an airstream, m/s
Q	–	heat transfer rate, W
X_f	–	length of the air side section inside the fin, mm
$X_{f\,\mathrm{in}}$	–	length of the air inlet section to the fin, mm
$X_{f\,\mathrm{out}}$	–	length of the air outlet section downstream of the fin, mm
X_{in}	–	length of the air inlet section, mm
X_{out}	–	length of the air outlet section, mm
ΔT	–	cooling effect in the airstream, $= T_{\mathrm{in}} - T_{\mathrm{out}}$, K
ΔT_{ln}	–	logarithmic mean temperature difference, K
Δp	–	pressure drop in the airstream, $= p_{\mathrm{in}} - p_{\mathrm{out}}$, Pa

Greek symbols

δ	–	characteristic dimension (L_p), m
ρ	–	air density, kg/m^3
λ_{air}	–	thermal conductivity of air, W/(m K)
ν	–	air kinematic viscosity, m^2/s
η	–	surface efficiency

Abbreviations

CFD	–	computational fluid dynamics
MCHE	–	minichannel heat exchanger

www.czasopisma.pan.pl PAN POLSKA AKADEMIA NAUK www.journals.pan.pl

1 Introduction

Nowadays, refrigeration systems face new challenges caused by environmental standards. According to the Regulation of the European Parliament and the Council of EU No. 517/2014, developed countries are obliged to reduce greenhouse gas emissions by about 80–95% by 2050 in comparison to 1990. The fluorinated greenhouse gases on the market should be reduced by about 79% by 2030. These actions were undertaken to prevent climate change. Conventional refrigerants are replaced by new ones with an indifferent impact on the environment. This situation is also a challenge for components of refrigeration systems, like heat exchangers (evaporators and condensers). A minichannel heat exchanger (MCHE) meets these requirements. MCHE is a type of heat exchanger, built from flat tubes with minichannels and louvered fins. Minichannels improve refrigerant heat transfer by enhancing the contact area. Furthermore, louvers on the fin wall improve air heat transfer by decreasing boundary layer thickness. MCHE is made from aluminum. Due to these features, it achieves high thermal performance. MCHE is applied in the automotive industry and is more frequently used in modern refrigeration systems because of its high effectiveness. In previous years, this device was the subject of many papers focused on its exploitation and the methods of construction improvement.

A good example of experimental studies was presented by Boeng *et al.* from the Federal University of Santa Catarina [1]. They performed experimental research on a new microchannel evaporator design for 'no frost' household refrigerators (sixteen aluminum evaporator samples). The researchers prepared empirical correlations based on the entire data set for the Colburn factor (j) and friction factor (f). They were able to predict 90% of the experimental data within ±10% and ±20% error bounds, respectively. Considering the air-side pressure drop observed for all microchannel evaporators tested, the authors concluded that such technology seems to be suitable for household refrigerating appliances as it barely impacts the total air flow rate of the system. Another case of the MCHE studies was conducted by Huang *et al.* [2]. The thermal and hydraulic performance of a designed compact bare-tube heat exchanger prototype was experimentally evaluated in comparison with the louvered-fin and flat-tube heat exchanger (with a similar frontal surface). Based on the experimental results it was possible to show that the bare tube heat exchanger was able to achieve the same heat capacity with 72% less envelop volume and 70% less material volume than in the case of louvered-fin and flat-tube heat exchangers. As

www.czasopisma.pan.pl PAN POLSKA AKADEMIA NAUK www.journals.pan.pl

regards the j/f ratio, the so-called coefficient of goodness, the value of the bare tube heat exchanger was 50% larger than that of the reference heat exchanger. Srisomba *et al.* [3] published experimental results showing the effect of the operating conditions on the performance of a microchannel heat exchanger under wet surface conditions. The subject of studies was an aluminum microchannel heat exchanger with a multi-louvered fin and multi-port minichannels. The tests were performed on R-134a refrigerant. The conditions were as follows: the relative air humidity in the range between 45% and 80% and the air inlet temperature of 27, 30, and 33°C. The Reynolds numbers ranged between 128 and 166. In their paper, the authors showed that when air inlet temperature and inlet relative humidity increase the heat transfer coefficient increases, but the wet fin efficiency decreases rapidly. Dogan *et al.* [4] performed the experimental comparison of double- and triple-row multi-louvered fin heat exchangers. The tests were conducted under constant thermal conditions and with identical frontal areas and depths. The tests in the wind tunnel were conducted under transient and steady-state conditions. The Reynolds number calculated based on the louvered pitch was 275. Their results showed that the heat exchanger with double-row fins had a higher thermal performance in terms of NTU (number of transfer units) and effectiveness.

The examination of automotive air conditioning systems was presented by Prabakaran *et al.* [5]. They conducted tests for two operating states (dry bulb temperature 27°C; relative humidity 40% and dry bulb temperature 40°C; relative humidity 40%) for the basic circuit (conventional serpentine evaporator with parallel flow condenser) and the enhanced (minichannel evaporator with an integrated receiver-dryer condenser). For both operating states, the coefficient of performance achieved in the test was higher for the enhanced cycle by 15% and 8%, respectively. The influence of the symmetrical and the asymmetrical pattern of the louvered fins was investigated experimentally by Vasi *et al.* [6]. The results of their work showed that the symmetrical setting of the louvers increases the values of heat transfer coefficients by 9.3% while reducing the pressure loss by 18.2% compared to the asymmetric setting. Additionally, with the set constant values of heat exchange and pressure drop for both settings, a 17.6% decrease in the weight of lamellas with symmetrical cuts can be observed. The next example of the test of compact heat exchangers with louver fins was presented by Ribeiro *et al.* [7]. They used wavy turbulators with louvers in the tubes and performed the experimental investigation for Reynolds numbers within the range 2588–7045. A new correlation for the Nusselt number in terms of

www.czasopisma.pan.pl PAN POLSKA AKADEMIA NAUK www.journals.pan.pl

the hydraulic diameter based Reynolds number, Prandtl number, and geometric parameters has been proposed for the tubes with turbulators. They observed a gain in the performance by use of the turbulators, obtained by a significant improvement in the convection heat transfer coefficient at the cost of an increase in the friction coefficient. Ayad *et al.* [8] investigated experimentally the air-side thermal-hydraulic performance of louvered fin and flat-tube heat exchangers under dehumidifying conditions. The tested louvered heat exchanger was characterized by geometrical dimensions as a flow depth of 47 mm, a high louver angle of 50°, and a louver pitch of 1.1 mm. The heat exchanger was tested in dry and wet work conditions. They observed that, for all inlet conditions, the wet friction factor is higher than that for the dry surface (from 15 to 43%). At a low Reynolds number, the Colburn factor under wet conditions is not influenced by the inlet humidity and it does not deviate from the dry conditions. However, as the Re increases, the sensible wet j factor decreases (up to 23%) compared to the dry one. Cao *et al.* [9] investigated the condensation heat transfer and pressure drop characteristics of R600a in a multi-louvered fins compact heat exchanger. The experiments conditions included saturation pressures from 530 to 620 kPa, mass fluxes from 25 to 41.25 kg/(m^{2}s), air temperature from 25 to 35°C, and inclined angles from 0° to 180° in horizontal and vertical directions, respectively. Based on the results, the authors noted that both the heat transfer capacity and the heat transfer coefficient of the condenser increase with an increase in mass flux. The heat transfer coefficient increases with the decrease in air temperature and the decrease in saturation pressure. However, both these parameters have opposite effects on the heat transfer capacity.

The computational fluid dynamics (CFD) methods are widely used in studies on MCHE performance. Yue *et al.* [10] used numerical simulations to evaluate MCHE heat transfer characteristics and flow mechanisms under different filling ratios in the evaporator of a microchannel separate heat pipe. The model was built in the Ansys Fluent software and it was validated in the experimental facility. The authors noticed that the optimal refrigerant filling ratio was from 68% to 100%. They found that the cooling capacity increased with the filling ratio and was as high as 4087 W at a filling ratio of 78%. They also noticed that the distribution of wall temperature and the liquid fraction both indicated that the effective heat transfer area of the two-phase region was a key parameter affecting the cooling capacity. Another numerical investigation of the louvered fin heat exchanger was developed by Zuoqin *et al.* [11]. They investigated the influence of louver fin

www.czasopisma.pan.pl PAN POLSKA AKADEMIA NAUK www.journals.pan.pl

configurations on thermal performance. The analyzed ranges of the geometry parameters were 7.5–12.5 mm (louver length, L_l), 8–20° (louver angle, L_a), and 2.25–3.75 mm (louver pitch, L_p). The achieved range of Reynolds number was 70–350. The authors showed the optimized geometrical parameters as $L_l = 7.5$ mm, $L = 8°$, and $L_p = 2.25$ mm. The best geometry increased the value of performance evaluation criterion by 19% in comparison to the reference one. Numerical studies on the air-side thermal-hydraulic performance of multi-louvered fin heat exchangers at Reynolds numbers from 30 to 500 were presented by Saleem and Kim [12]. The authors conducted parametric studies for 36 heat exchanger configurations with louver angles between 19–31°, fin pitches of 1.0, 1.2, and 1.4 mm, and flow depths of 16, 20, and 24 mm. They determined numerically the critical Reynolds number and the variation in flow physics along with the thermal and hydraulic performance of the microchannel heat exchanger. The researchers found that the critical Reynolds number rises with an increase in flow depth (F_d) and a decrease in fin pitch (F_p) values. Based on the heat transfer coefficient determined using numerical results, they reported the best air-side thermal performance for geometry with $F_p = 1$ mm, $F_d = 16$ mm, and $L_a = 19°$. The other example of the numerical investigation of the louvered fin was provided by Shinde *et al.* [13]. They conducted numerical studies of aluminum heat exchangers with different fin and tube geometrical configurations in the range of Reynolds numbers from 25 to 200. Three different heat exchanger geometries were obtained for the experimental investigation purposes with constant fin pitch (14 fins per inch) but varied fin geometrical parameters (fin height, fin thickness, louver pitch, louver angle, louver length, and flow depth) were numerically investigated. The research team found that in the tested range of small Reynolds numbers, the flow is directed by fin instead of louvers. Karthik *et al.* [14] also provided a parametric analysis of the performance of a compact heat exchanger using numerical methods. The researchers modeled different frontal air velocities by changing the geometrical parameters such as fin pitch, transverse tube pitch, longitudinal tube pitch, louver pitch, and louver angle. The authors found that a decrease in fin pitch led to a higher pressure drop at a tested frontal air velocity. The effect of the increase in both transverse and longitudinal tube pitches resulted in a higher pressure drop due to an increase in the surface without louvers. The influence of these parameters on the convective heat transfer coefficient is very minimal owing to the constant of the louver configuration. The reduction of the louver pitch contributed to a higher pressure drop with only a minimal increase in heat transfer

www.czasopisma.pan.pl PAN POLSKA AKADEMIA NAUK www.journals.pan.pl

coefficient and hence, the goodness factor of the compact heat exchanger decreased significantly. An example of the numerical investigations concerning the methods for enhancement of MCHE performance was presented by Dezan *et al.* [15]. The influence on the thermal efficiency of two geometries with a vortex generator was investigated. The geometrical differences concerned the louver height and delta-winglet frontal area. The Reynolds numbers based on the hydraulic diameter of 120 and 240 were tested. The calculation was conducted using Ansys Fluent. The authors stated that for both geometries and Reynolds numbers, the louver angle is the major contributor to the friction factor. Another numerical test was presented by Kang's research group [16] who examined a prototype minichannel heat exchanger working with fuel cells. The heat exchanger was investigated in terms of achieved heat transfer rates on the air side and pressure drops. The authors commented that the arrangement of pipes in the prototype had little effect on the pressure drop but had a large impact on the heat transfer coefficient due to the contact zone of the pipes and the lamellas with the louvers. Martinez-Ballester *et al.* [17] investigated the effect of the number of passes of the medium in the heat exchanger on its operation. They found that there is an optimal value of the number of passes, in the case studied, it was 3. With such a number, they noticed an increase in heat exchange of approx. 3%. The numerical and analytical approach to condensation in MCHE was presented by Kumar's research team [18]. The authors used an analytical approach to calculate the heat transfer and the pressure drop through the condenser. In the analytical approach, the condenser was discretized into multiple segments and the effectiveness of heat exchanger – number of heat transfer unit (ε-NTU) method was applied. In the second approach, computational fluid dynamics was used to analyze condensation phenomena inside the microchannel and it was compared with the analytical results. The maximum deviation of the heat transfer and the internal pressure drop (refrigerant side) for the analytical approach was found to be 8.3% and 9.4%, respectively compared to the experimental results. The results showed that the proposed analytical approach can be used to calculate the heat rejection and internal (refrigerant) pressure drop within the 10% accuracy range.

The literature review shows that most of the experimental and numerical research was performed for Reynolds numbers in the range of 25–500. The numerical research concerns geometrical parameters of fins, for example, fin height, fin pitch, louver pitch, louver height, etc. However, there is a lack of data due to the influence of louver height on thermal performance.

www.czasopisma.pan.pl PAN POLSKA AKADEMIA NAUK www.journals.pan.pl

The present work focuses on the numerical investigation of minichannel heat exchangers with different louver heights based on the results from an experimental study conducted on the small heat pump system test rig. The tests were performed in the range of Reynolds numbers from 93 to 486. The *JF* factor was used to determine the performance of each geometry.

2 Materials and methods

The object of the tests was the MCHE with rectangular fins (shown in Fig. 1), which was working as an evaporator in a small refrigeration system (Fig. 2).

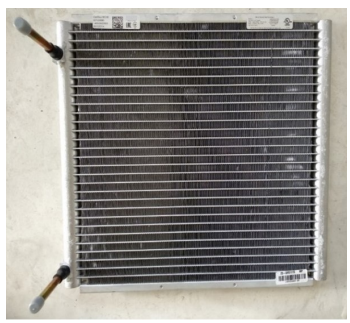

Figure 1: Tested minichannel heat exchanger.

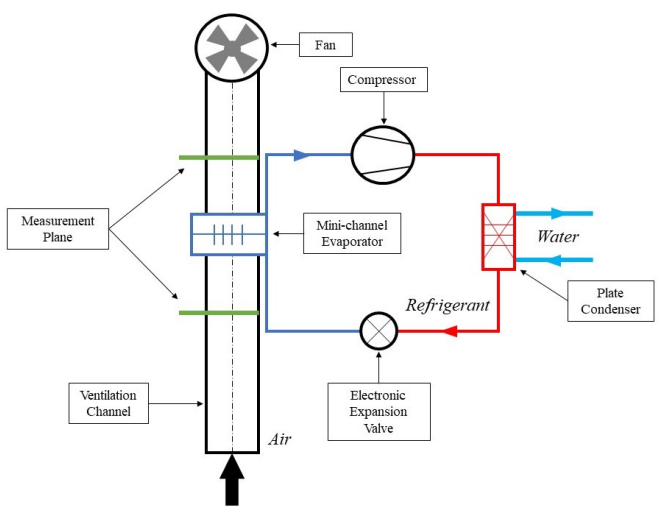

Figure 2: Scheme of the experimental stand of small air heat pump system.

www.czasopisma.pan.pl PAN POLSKA AKADEMIA NAUK www.journals.pan.pl

The experimental rig consisted of two parts: a refrigeration system and a ventilation channel. The refrigeration system consists of a scroll compressor, water cooled plate condenser, an electronic expansion valve (EEV), and a tested minichannel evaporator. By controlling the parameters of the refrigeration system (rotation speed of the compressor, stream of water in the condenser, and percentage of opening of EEV), the evaporating conditions in MCHE can be adjusted. The second part of the experimental rig is the ventilation channel in which the tested MCHE evaporator is placed. The airflow through the channel is forced by a fan placed at the outlet of the channel. Evaluation of MCHE performance was based on the measurement of airflow parameters in the ventilation channel. These parameters included the mean velocity of the airflow in front of MCHE, the pressure drop through the heat exchanger, and the temperature distribution before and after the evaporator. The locations of the measurement points inside the ventilation channel with the dimensions are presented in Fig. 3.

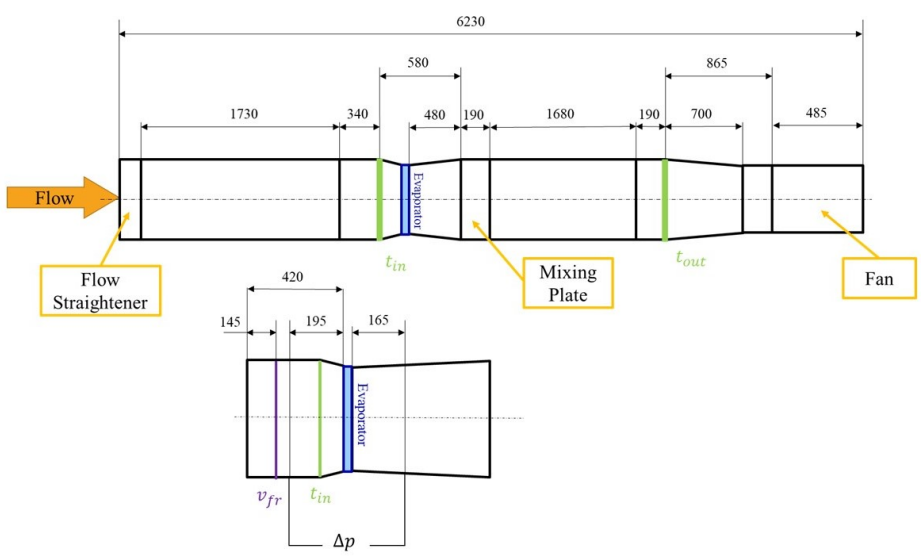

Figure 3: Scheme of ventilation channel with the location of measurement points.

The experimental rig was described in the previous paper [19]. The rig was improved by changing the expansion element and improvement of the air velocity measurement system. A change of the expansion element was implemented in the way to acquire a higher range of the evaporator capacity control. Thus, the electronic expansion valve Carel E2V 14BSF01 and Carel

www.czasopisma.pan.pl PAN POLSKA AKADEMIA NAUK www.journals.pan.pl

EVD controller were used. To enhance the accuracy of velocity measurement, a tungsten hot-wire probe with module ATU-08 was implemented in place of the previously used climate meter. Additionally, the ventilation channel was equipped with a flow straightener and a mixing plate. Both elements were used according to the improvement of the airflow parameters.

3 Numerical methods

The numerical model was based on the dimensions of the real object. The analysis concerned air flow inside one of the louvered fins (Fig. 4). The model of the fin consisted of one fin and two flat tubes on the bottom and top (half of the thickness). The schematic drawing of the louvered fin and the dimensions are shown in Fig. 5 and Table 1.

Figure 4: The geometrical model of the tested louvered fin.

Table 1: The dimensions of the tested louvered fin.

F_d	F_p	H	L_l	L_p	L_a
15.8 mm	0.95 mm	8 mm	1.1 mm	1.13 mm	20°

The louvered height (L_h) was the parameter changed in the analysis. The simulations were performed for heights: 0, 1.5, 2.5, 3.5, 4.5, 5.5, 6.5, and 7 mm. The reference value of the louver height in the real object was 6.5 mm. The simulations with a 1 mm step were performed to the minimal value of 1.5 mm. Moreover, the simulations for 0 and 7 mm (0 mm is plain fin and 7 mm is the maximum height due to geometrical construction) were additionally carried out.

www.czasopisma.pan.pl PAN POLSKA AKADEMIA NAUK www.journals.pan.pl

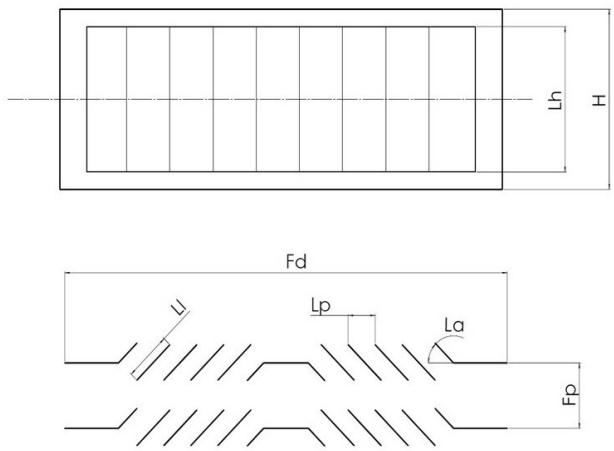

Figure 5: The schematic diagram of the tested louvered fin: H – fin height, L_h – louver height, F_d – flow depth, F_p – fin pitch, L_l – louver length, L_p – louver pitch, L_a – louver angle.

The analyzed geometry consisted of two domains: solid and fluid. The solid domain is the aluminum fin. The fluid domain is the air stream flowing through the fin. The air is modeled as an ideal gas. The thermodynamic properties of both domains are presented in Table 2. To obtain a well-distributed mesh the fluid domain was divided into five parts. The ge-

Table 2: Thermodynamic properties of the domains.

Parameter	Value
Air molar mass	$28.96\ \frac{\text{kg}}{\text{kmol}}$
Air density	$1.185\ \frac{\text{kg}}{\text{m}^3}$
Air specific heat	$1004.4\ \frac{\text{J}}{\text{kg}\cdot\text{K}}$
Pressure	101.325 Pa
Air dynamic viscosity	$1.5\cdot 10^{-5}\ \frac{\text{kg}}{\text{m}\cdot\text{s}}$
Air thermal conductivity	$2.61\cdot 10^{-2}\ \frac{\text{W}}{\text{m}\cdot\text{K}}$
Aluminum thermal conductivity	$237\ \frac{\text{W}}{\text{m}\cdot\text{K}}$

www.czasopisma.pan.pl PAN POLSKA AKADEMIA NAUK www.journals.pan.pl

ometrical model and its schematic view are displayed in Figs. 6 and 7, respectively. The dimensions are described in Table 3.

Table 3: Dimensions of the air domain sections.

X_{in}	$X_{f\,\text{in}}$	X_f	$X_{f\,\text{out}}$	X_{out}
8 mm	1.9 mm	16 mm	1.9 mm	48 mm

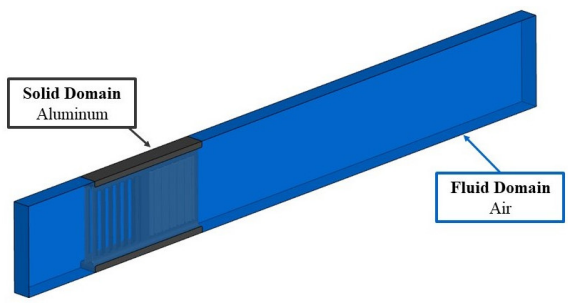

Figure 6: The geometrical model of the tested louvered fin.

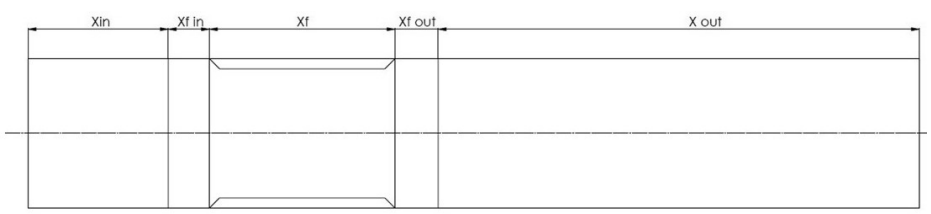

Figure 7: Schematic view of the division of air domain: X_{in} – inlet section, $X_{f\,\text{in}}$ – inlet section to the fin, X_f – fin section, $X_{f\,\text{out}}$ – outlet section downstream of the fin, X_{out} – outlet section.

After the design of the domain geometry, the mesh density independence test was performed. For 8 different densities of each grid, two simulations were conducted, for 1 and 5 m/s (minimum and maximum flow). Based on the calculation results the mesh with 2 412 583 elements was chosen which made it possible to achieve the required accuracy of the results while maintaining a reasonable calculation time.

The numerical model was used to simulate the phenomenon of heat transfer during air cooling by the fragment of MCHE. The measured value of air temperature and velocity at the inlet to the channel was set on the

www.czasopisma.pan.pl PAN POLSKA AKADEMIA NAUK www.journals.pan.pl

Inlet surface. On the *Outlet* surface, the relative pressure was set at 0 Pa. In the horizontal direction, the translation periodicity was used for the fluid and the solid domains. Therefore, the right position of the louvers could be established. Additionally, on the top and bottom surfaces of the fin (purple surfaces in Fig. 8), the boundary *Wall* of constant temperature was set. For experiment validation, the values of the inlet velocity and temperatures were taken from the test conditions but in the case of parametric simulation, the values of these parameters were set. All boundaries with their location are presented in Fig. 8 and the values of each set parameter are summarized in Table 4. In the table, the parameter values are divided into two sections: the validation model (where there are parameter values entered into the numerical model from the experiment condition) and the parametric model

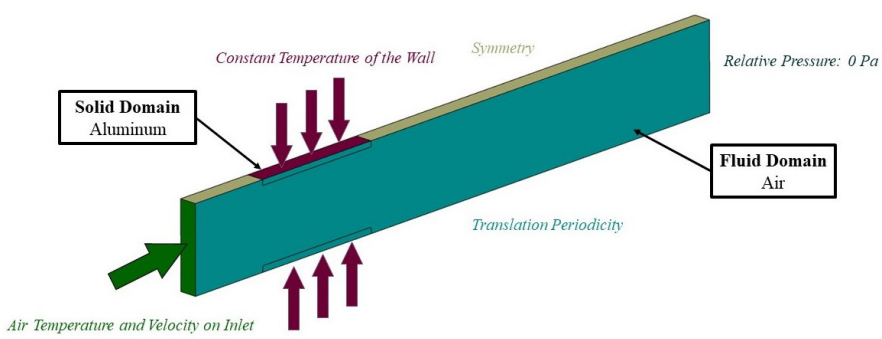

Figure 8: Boundary conditions distribution.

Table 4: Parameters used in simulation.

Parameter	Validation model	Parametric model
Temperature on the surface (*Inlet*), K	293.55 293.45 292.85 292.45	298.15
Temperature on the solid boundary (*Wall*), K	288.05 289.05 289.15 289.45	288.15
Velocity on the surface (*Inlet*), m/s	0.86 1.67 2.48 3.29	1 2 3 4 5
Relative pressure, Pa	0	0

www.czasopisma.pan.pl PAN POLSKA AKADEMIA NAUK www.journals.pan.pl

(where there are conditions for numerical analysis of the impact of the louver height on the efficiency).

The simulations were conducted in *Ansys CFX 2021 R1* [22] with the following solver settings: a first-order turbulence model and an *SST k-ω* model of turbulence. The convergence criterion for the momentum and heat transfer was 10^{-6}.

The validation of the CFD model for the louver height of 6.5 mm (louver height for tested MCHE) is shown in Fig. 9, where a cooling effect and pressure drop are presented. Additionally, Table 5 lists the maximum values of estimated measurement uncertainties.

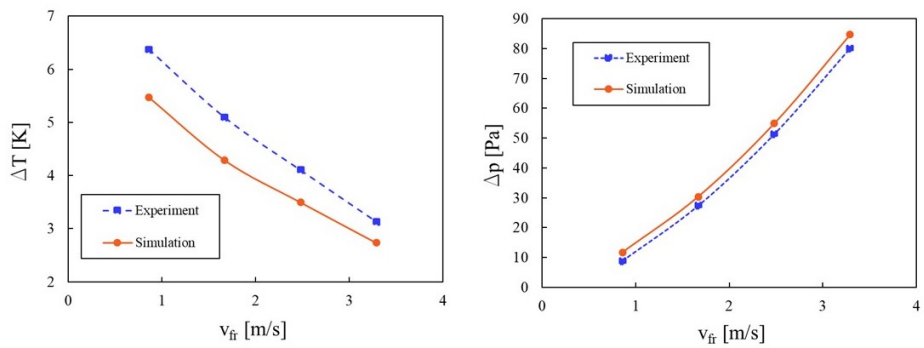

Figure 9: Validation of the simulation: the cooling effect (left picture) and the pressure drop (right picture) *vs.* the mean value of the frontal velocity of the airstream.

Table 5: The measurement uncertainties.

Parameter	Maximum value of uncertainty
Mean value of the frontal velocity of an airstream, v_{fr}	0.1 m/s
Pressure drop in the airstream, Δp	0.74 Pa
Cooling effect in the airstream, ΔT	0.4 K

The tested numerical approach compared with the experimental results is shown in Fig. 9. The cooling effect convergence is within the range of 12.8–15.8%. The differences are probably caused by the temperature in the flow channels of MCHE. The refrigerant distribution in minichannels is non-uniform, which could be caused by occlusion. The dimensions of minichannels are rather small, and they may be easily clogged with solid

www.czasopisma.pan.pl PAN POLSKA AKADEMIA NAUK www.journals.pan.pl

impurities (for example from soldering). That phenomenon can disrupt the proper, uniform distribution of heat transfer in the contact area between the air and the aluminum flat tube. This condition raises uncertainty in the calculation of the average temperature of the fin. In terms of pressure loss, the convergence is in the range between 5.8–32.7%. The highest value of convergence was noted for the minimum velocity of the air stream (0.86 m/s), and the lowest value for the maximum velocity of the air stream (3.29 m/s). The measurement error in the case of pressure drop is constant. In other words, it had the biggest influence on the smallest measured value of pressure loss.

4 Results and discussion

Characteristics concerning changes in the pressure drop and the cooling effect with the change in the mean frontal velocity of the airstream are shown in Fig. 10. One can see that pressure drop increases with the velocity of the airflow (Fig. 10, right), and the highest values are achieved for a louver height of 7 mm. The highest value of pressure drop achieved in the test is approx. 120 Pa. As regards the cooling effect (Fig. 10, left), it is decreasing with increasing velocity of the airflow. It can be observed that the highest values of the cooling are achieved for the maximum considered louver height. One can notice that there is a linear trend of the characteristics in the range of louver height within 5.5–7 mm. The highest value of the cooling effect achieved in the test is almost 10 K.

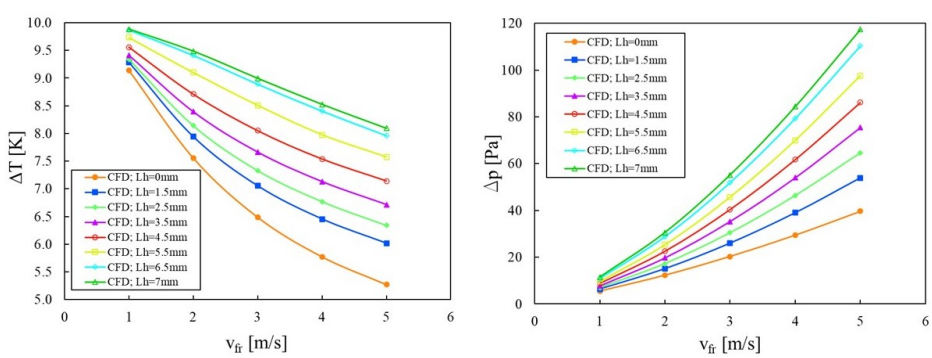

Figure 10: The influence of the mean value of the frontal airflow velocity on the cooling effect (left picture) and the pressure drop (right picture).

www.czasopisma.pan.pl PAN POLSKA AKADEMIA NAUK www.journals.pan.pl

Further analysis was based on dimensionless numbers. The friction factor (f) and Colburn j factor were used to describe pressure drop and heat transfer. Both coefficients were presented as the function of the Reynolds number.

The Re based on the louver pitch (L_p) is calculated according to the formula [20]

$$\mathrm{Re}_{L_p} = \frac{v_{\mathrm{ave}}\delta}{\nu}\,, \tag{1}$$

where v_{ave} is the mean value of airstream velocity in the MCHE channel, δ represents the characteristic dimension ($\delta = L_p$), and ν is the air kinematic viscosity.

The Colburn and friction factors are given by, respectively:

$$j = \frac{\eta h \mathrm{Pr}^{2/3}}{\rho v_{\mathrm{ave}} c_p}\,, \tag{2}$$

$$f = \frac{2\Delta p}{\rho v_{\mathrm{ave}}^2}\frac{A_c}{A}\,, \tag{3}$$

where ρ and c_p are the density and specific heat of air, respectively, Δp denotes the pressure drop, A is the airside area of the heat exchanger, A_c represents the minimum free flow area of a heat exchanger, η is the surface efficiency, and Pr is the Prandtl number.

The heat transfer coefficient is defined as

$$h = \frac{Q}{A\Delta T_{ln}}\,, \tag{4}$$

where ΔT_{ln} is the logarithmic mean temperature difference and Q is the heat transfer rate.

The range of Reynolds numbers for the experiment is from 93 to 486. The friction factor for the tested geometries varies from 0.050 to 0.300 (Fig. 11, right). The characteristics show that higher louver height means a higher friction factor. In terms of the j factor (Fig. 11, left), one can observe a similar trend. But the values for louver height ranging from 0 to 4.5 are characterized by smaller differences of j factor values than in the case of other tested cases. The highest j values are obtained for 7 mm.

Additionally, based on the simulation results, the Nusselt numbers (based on the louver pitch as the characteristic dimension) were calculated using the formula

$$\mathrm{Nu}_{L_p} = \frac{h\delta}{\lambda_{\mathrm{air}}}\,, \tag{5}$$

www.czasopisma.pan.pl PAN POLSKA AKADEMIA NAUK www.journals.pan.pl

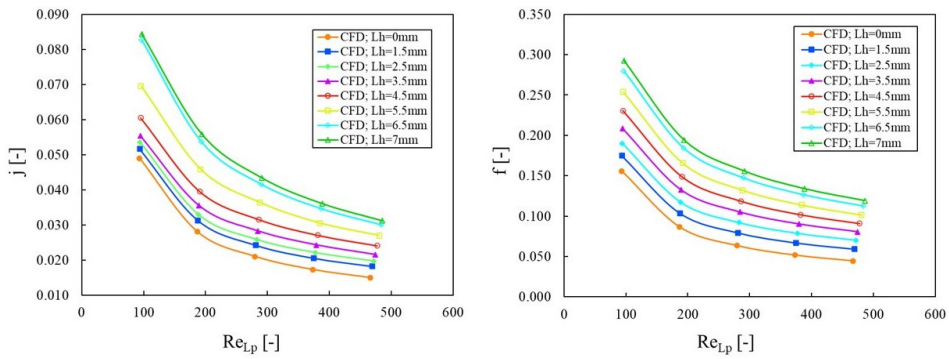

Figure 11: Characteristics of the Colburn factor (left picture) and the friction factor (right picture) *vs.* Reynolds number.

where λ_{air} is the thermal conductivity of air, and $\delta = L_p$. The characteristics of this parameter are shown in Fig. 12. The values of the Nusselt number increased with the increase in louver height. Under the tested conditions the Nusselt number was in the range from 4 to 13.

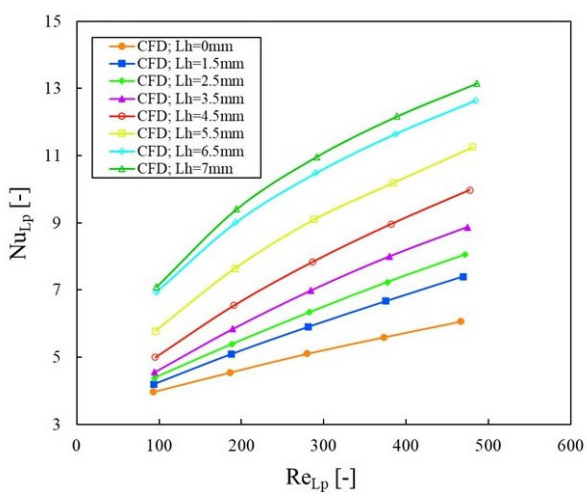

Figure 12: Characteristics of the Nusselt number *vs.* Reynold number.

The evaluation of the effectiveness is conducted based on the *JF* factor. This parameter refers to the heat transfer and the pressure drop in the

www.czasopisma.pan.pl PAN POLSKA AKADEMIA NAUK www.journals.pan.pl

airflow and is calculated using the formula [21]:

$$JF = \frac{\dfrac{j}{j_{\mathrm{ref}}}}{\sqrt[3]{\dfrac{f}{f_{\mathrm{ref}}}}}, \tag{6}$$

where j_{ref} and f_{ref} represent the Colburn and friction factors for the reference geometry, respectively. In the present study, the reference geometry is the fin with $L_h = 0$ mm. The values of the JF factor are compared with the reference geometry.

The characteristics of the JF factor variable with the mean value of the frontal velocity of the airstream are shown in Figure 13. As one can see, the first two values of louver height (1.5 and 2.5 mm) improved effectiveness by a maximum of about 0.13. The trends of their changes are similar. The maximum value of JF was obtained for the largest airflow velocity, but for the velocity of 1 m/s, there is almost no growth at all. The geometry with the louver height of 3.5 mm shows better performance but only a slight

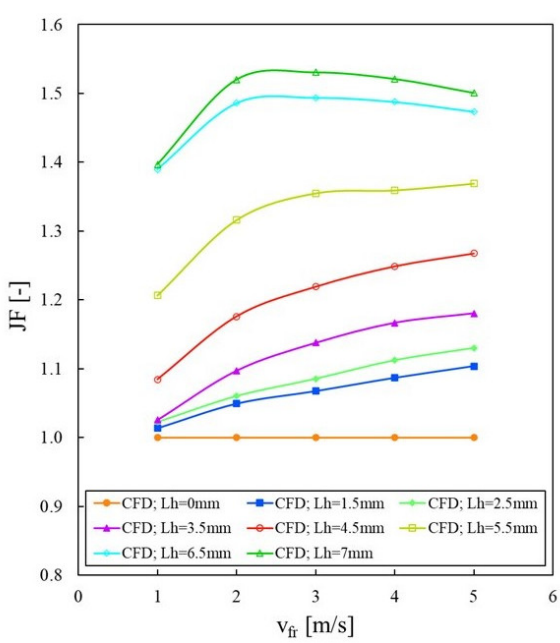

Figure 13: Characteristics of JF factor *vs.* the mean value of the frontal velocity of airstream.

www.czasopisma.pan.pl PAN POLSKA AKADEMIA NAUK www.journals.pan.pl

improvement for small velocity (1 m/s). The maximum enhancement is observed for 5 m/s airflow ($JF = 0.181$). Next geometry ($L_h = 4.5$ mm) increased the value of JF in the range of 0.084 to 0.267. The improvement was achieved in the whole examined range of airflow velocity. A similar situation is in the case of geometry with $L_h = 5.5$ mm. The performance increased in the whole velocity range and the value of JF enhancement is from 0.206 to 0.369. The two last geometries, i.e., with louver heights of 6.5 mm (real object L_h) and 7 mm, show a similar trend. The effectiveness improved in a whole range of tested velocities and the maximum value was achieved for 3 m/s. The maximum JF improvement is observed for 7 mm geometry for the velocity of 3 m/s and it is 0.531.

Figure 14 demonstrates the effect of airflow velocity on the JF factor depending on the louver height. The trend of improvement for each height is similar but it is the worst for the velocity of 1 m/s. For this velocity, the improvements can be noted for L_h larger than 3.5 mm. The best performance is achieved for the maximum value of L_h at the velocity of 3 m/s. It can be explained by an occurrence of a flow regime in which the flow is driven by louvers, but there is a smaller pressure drop than in the case of the highest velocity. This is the reason why this area of exploitation ($L_h = 7$ mm; $v_{fr} = 3$ m/s) brings better effects.

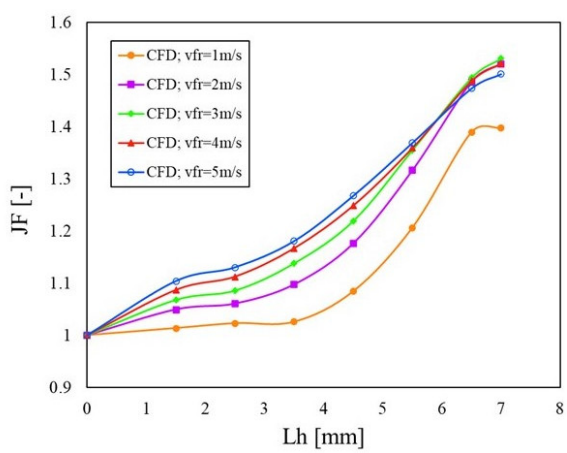

Figure 14: Characteristics of JF factor *vs.* louver height.

Figures 15 and 16 show the comparison of velocity and temperature distribution, respectively, in the air domain for $L_h = 0$ mm and 7 mm (minimum and maximum height). The comparison is based on the parameters' distri-

www.czasopisma.pan.pl PAN POLSKA AKADEMIA NAUK www.journals.pan.pl

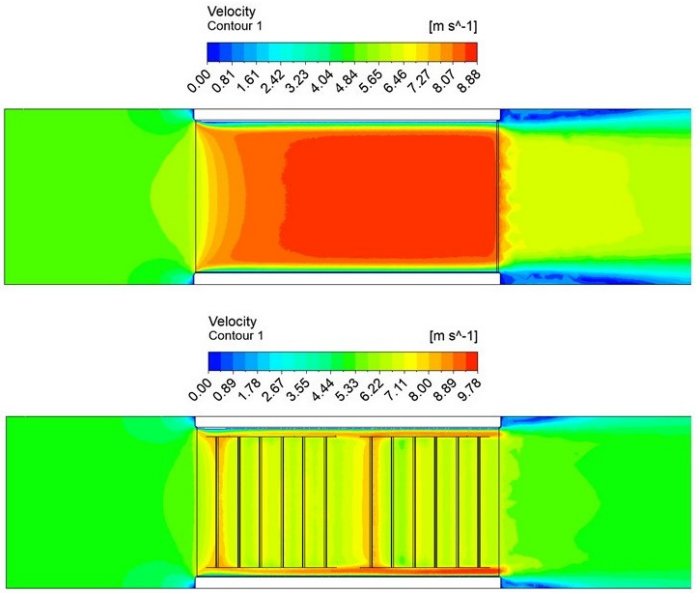

Figure 15: Distribution of velocity inside the air channel of MCHE: $L_h = 0$ mm (top), $L_h = 7$ mm (bottom).

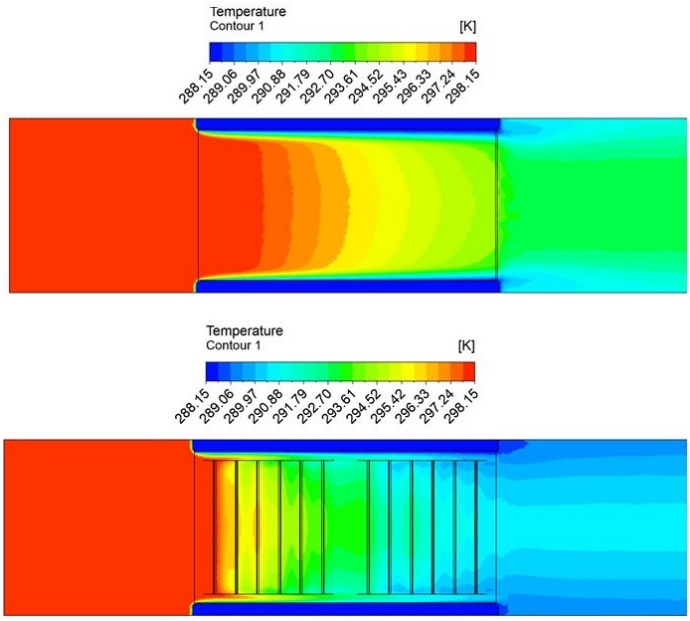

Figure 16: Distribution of temperature in the air channel of MCHE: $L_h = 0$ mm (top), $L_h = 7$ mm (bottom).

www.czasopisma.pan.pl PAN POLSKA AKADEMIA NAUK www.journals.pan.pl

bution on the vertical plane in the center of the air channel in the flow direction, obtained for 5 m/s inlet velocity. The influence of louvers on the velocity distribution can be observed in Fig. 15. For the maximum velocity of the air stream (5 m/s), the area of maximum velocity for the plain fin geometry is much wider than for the highest louver case (7 mm). Additionally, the area of vortex below the flat tube is better observable in the plain fin. As for the temperature distribution, faster cooling can be noticed at the maximum louver height ($L_h = 7$ mm, Fig. 16 (bottom picture)). A cooling effect similar to the plate fin is observed in the half-length of the flow channel.

5 Conclusions

- The effectiveness of the cooling is rising with an increase of L_h.
- In terms of the JF factor, the highest value was achieved in the tested range for geometry with the maximum louver height ($L_h = 7$ mm).
- The best performance is achieved in the range of 2–4 m/s, where there are smaller pressure drops and louver-directed flow of the medium.

Acknowledgements

This paper has been completed while the first and second authors were Doctoral Candidates in the Interdisciplinary Doctoral School at the Lodz University of Technology, Poland.

Received 8 March 2023

References

[1] Boeng J., Marcon A.A., Hermes C.J.L.: *Air-side heat transfer and pressure drop characteristics of microchannel evaporators for household refrigerators*. Int. J. Heat Mass Transf. **147**(2020), 2, 118913.

[2] Huang Z., Ling J., Hwang Y., Aute V., Radermacher R.: *Airside heat transfer and friction characteristics of a 0.8 mm diameter bare tube heat exchanger*. Heat Transf. Eng. **41**(2019), 8, 1–11.

[3] Srisomba R., Asirvatham L.G., Mahian O., Dalkilic A.S., Awad M.M., Wongwises S.: *Air-side performance of a micro-channel heat exchanger in wet surface conditions*. Therm. Sci. **21**(2017), 1, 375–385.

www.czasopisma.pan.pl PAN POLSKA AKADEMIA NAUK www.journals.pan.pl

[4] Dogan B.I., Altun Ö., Ugurlubilek N., Tosun M., Sariçay T., Erbay L.B.: *An experimental comparison of two multi-louvered fin heat exchangers with different numbers of fin rows.* Appl. Therm. Eng. **91**(2015), 12, 270–278.

[5] Prabakaran R., Dhasan L.M., Prabhakaran A., Jha K.K.: *Experimental investigations on the performance enhancement using minichannel evaporator with integrated receiver-dryer condenser in an automotive air conditioning system.* Heat Transf. Eng. **40**(2018), 2, 667–678.

[6] Vaisi A., Esmaeilpour M., Taherian H.: *Experimental investigation of geometry effects on the performance of a compact louvered heat exchanger.* Appl. Therm. Eng. **31**(2011), 11, 3337–3346.

[7] Ribeiro F., de Conde K., Garcia E.C., Nascimento I.P.: *Heat transfer performance enhancement in compact heat exchangers by the use of turbulators in the inner side.* Appl. Therm. Eng. **173**(2020), 6, 115188.

[8] Ayad F., Benelmir R., Idris M.: *Thermal-hydraulic experimental study of louvered fin-and-flat-tube heat exchanger under wet conditions with variation of inlet humidity ratio.* Appl. Therm. Eng. **183**(2021), 1, 116218.

[9] Cao X., Wang X., Song Q., Wang D., Li Y.: *Experimental investigation on the heat transfer and pressure drop characteristics of R600a in a minichannel condenser with different inclined angles.* Appl. Therm. Eng. **196**(2021), 9, 117227.

[10] Yue C., Zhang Q., Zhai Z., Ling L.: *CFD simulation on the heat transfer and flow characteristics of a microchannel separate heat pipe under different filling ratios.* Appl. Therm. Eng. **139**(2018), 7, 25–34.

[11] Qian Z., Wang Q., Cheng J., Deng J.: *Simulation investigation on inlet velocity profile and configuration parameters of louver fin.* Appl. Therm. Eng. **138**(2018), 6, 173–182.

[12] Saleem A., Kim M.H.: *CFD analysis on the air-side thermal-hydraulic performance of multi-louvered fin heat exchangers at low Reynolds numbers.* Energies **10**(2017), 6, 823.

[13] Shinde P., Schäfer M., Lin C.: *Numerical investigation of micro-channeled louver fin aluminum heat exchangers at low Reynolds number.* ASME 2016 Heat Transfer Summer Conf., Washington 2016.

[14] Karthik P., Kumaresan V., Velraj R.: *Experimental and parametric studies of a louvered fin and flat tube compact heat exchanger using computational fluid dynamics.* Alex. Eng. J. **54**(2015), 4, 905–915.

[15] Dezan D.J., Salviano L.O., Yanagihara J.I.: *Interaction effects between parameters in a flat-tube louvered fin compact heat exchanger with delta-winglets vortex generators.* Appl. Therm. Eng. **91**(2015), 12, 1092–1105.

[16] Kang H., Hyejung C., Kim J. H., Jacobi A.M.: *Air-side heat transfer performance of louver fin and multi-tube heat exchanger for fuel-cell cooling application.* J. Fuel Cell Sci. Technol. **11**(2014), 4, 041004.

[17] Martínez-Ballester S., Corberán J.M., Gonzálvez-Maciá J.: *Numerical model for microchannel condensers and gas coolers: Part II – Simulation studies and model comparison.* Int. J. Refrig. **36**(2013), 1, 191–202.

www.czasopisma.pan.pl PAN POLSKA AKADEMIA NAUK www.journals.pan.pl

[18] Kumar R., Vijayaraghavan S., Govindaraj D.: *Numerical and analytical approach to study condensation for automotive heat exchangers*. Mater. Today: Proc. **52**(2022), 3, 556–564.

[19] Kowalczyk M.J., Łęcki M., Romaniak A., Warwas B., Gutkowski A.N.: *Investigations of thermal-flow characteristics of minichannel evaporator of air heat pump*. Archiv. Thermodyn. **41**(2021), 4, 261–279.

[20] Kang H., Jun G.W.: *Heat transfer and flow resistance characteristics of louver fin geometry for automobile applications*. J. Heat Transf. **133**(2011), 10, 101802.

[21] Yun J.Y., Lee K.S.: *Influence of design parameters on the heat transfer and flow friction characteristics of the heat exchanger with slit fins*. Int. J. Heat Mass Transf. **43**(2000), 7, 2529–2539.

[22] Ansys, Inc. *Ansys CFX-Pre User's Guide*. 2021.